

PION FLUCTUATION IN HIGH-ENERGY COLLISIONS — A CHAOS-BASED QUANTITATIVE ESTIMATION WITH VISIBILITY GRAPH TECHNIQUE*

SUSMITA BHADURI, DIPAK GHOSH

Deepa Ghosh Research Foundation
60/7/1, Maharaja Tagore Road, Kolkata-700031, India
www.dgfoundation.in

(Received November 14, 2017; accepted March 16, 2017)

We propose a new approach for studying pion fluctuation for deeper understanding of the internal dynamics, from a perspective of fractional Brownian motion (fBm)-based complex network analysis method called Visibility Graph analysis. This chaos-based, rigorous, non-linear technique is applied to study the erratic behaviour of multipion production in π^- -Ag/Br interactions at 350 GeV. This method can offer reliable results with finite data points. The Power of Scale-freeness of Visibility Graph denoted by PSVG is a measure of fractality, which can be used as a quantitative parameter for the assessment of the state of a chaotic system. The event-wise fluctuation of the multipion production process can be represented by this parameter. From the analysis of the PSVG, we can quantitatively confirm that fractal behaviour of the particle production process depends on the target excitation, and the fractality decreases with the increase of target excitation.

DOI:10.5506/APhysPolB.48.741

1. Introduction

For the last decade, the analysis of large density fluctuations in high-energy interactions has received much attention due to its capability to provide information on the dynamics of the process of multiparticle production. A new method named intermittency was first introduced by Bialas and Peschanski [1] for the analysis of large fluctuations. The power-law behaviour of the factorial moments with respect to the size of phase-space intervals in decreasing mode has been detected in multipion production in heavy-ion interaction. This was indicative of self-similar fluctuation in this process.

* Funded by SCOAP³ under Creative Commons License, CC-BY 4.0.

In the recent past, several techniques based on the fractal theory have been used to analyse the multipion emission data [2–6]. Hwa and Takagi have developed the most popular of them — Gq moment and Tq moment [2, 6]. Considering their merits and demerits, both these methods have been extensively applied to analyse the multipion emission process [7, 8]. Then techniques like the Detrended Fluctuation Analysis (DFA) method [9] have been used for determining monofractal scaling parameters, and the Hurst exponent, which is related with fractal dimension, has been deduced from the DFA function of a time series [10]. The method has been used for detecting long-range correlations in noisy and non-stationary time-series data [11, 12]. DFA method has been extended by Kantelhardt *et al.* [13] for analysing non-stationary and multifractal time series. This generalized DFA is known as the multifractal-DFA (MF-DFA) method. Zhang *et al.* [14] applied MF-DFA method to analyse the multifractal structure of the distribution of shower particles around central rapidity region of Au–Au collisions at $\sqrt{s_{NN}} = 200$ A GeV. Multifractal analysis in particle production processes has been recently done in various works [15–19]. Both DFA and MF-DFA methods give most accurate results for random processes like the Brownian motion where the time series has an *infinite* number of data points. But in real-life situations, we hardly get infinite number of data points and end up using *finite* number of data points for calculation of the Hurst exponent and the MF-DFA parameter. In this process, the long-range correlations in the time series are fractionally broken into finite number of data points and the local dynamics relating to a particular temporal window are obviously overestimated.

In the recent past, Albert and Barabási have reviewed the latest advances in the field of complex network and discussed the analytic tools and models for random graphs, small-world and scale-free networks [20, 21]. Havlin *et al.* [22] have discussed the application of network sciences to the description, analysis, understanding, design and repair of multi-level complex systems which is detected in man-made and human social systems, in organic and inorganic matter, from nano- to macroscales, and in natural and anthropogenic structures. Zhao *et al.* [23] have investigated the dynamics of stock market by means of correlation-based network, and identified global expansion and local clustering market behaviours during crises using the heterogeneous time scales. In this regard, Visibility Graph analysis [24, 25] method has gained importance due to its entirely different, rigorous approach. Lacasa *et al.* have used fractional Brownian motion (fBm) and fractional Gaussian noises (fGn) series as a theoretical framework to analyse real-time series in different scientific fields. The Hurst parameter calculated for fBm with different methods, often yields ambiguous results, because of the presence of inherent non-stationarity and long-range dependence in fBm. Lacasa *et al.* [24, 25] applied classic method of complex network anal-

ysis to quantify long-range dependence and fractality of a time series [25] and mapped fBm and fGn series into a scale-free Visibility Graph having the degree distribution as a function of the Hurst exponent [25]. They have further analysed Q -series [26], Stern series [27] and Thue–Morse series [28], and showed that Visibility Graph can differentiate different kinds of complexity and fractality. Moreover, they have suggested that this algorithm not only detects the difference between random and chaotic series but also the spatial location of inverse bifurcations in chaotic dynamical systems. The reliability of Visibility Graph method has been confirmed for artificial data series as well as real data series by Lacasa *et al.* [24, 25] the details of which are given in [29, 30]. Visibility Graph analysis is altogether a new concept to estimate fractality from a new perspective without estimating multifractality. Moreover, this method has been applied widely over time series with *finite* number of data points, even with 400 data points [31], and has achieved reliable result in various fields of science. Zhao *et al.* have applied both MF-DFA and Visibility Graph methods to investigate the fluctuation and geometrical structures of magnetization time series and confirmed that the Hurst exponent is a good indicator of phase transition for a complex system [32]. Recently, we have analysed multiplicity fluctuation around the central rapidity and phase transition in high-energy interactions — one hadron–nucleus and other nucleus–nucleus, namely π^- -AgBr (350 GeV) and ^{32}S -AgBr (200 A GeV), using Visibility Graph method [33]. Further, using the same method, we have analysed the fractality of void probability distribution measured for pseudorapidity (η) and azimuthal angle (ϕ) space in ^{32}S -Ag/Br interaction at an incident energy of 200 GeV per nucleon [34–36].

Target protons, also known as grey tracks as per the terminology of nuclear emulsion, are the low-energy part of intra-cascade formed from high-energy interactions. It should be noted that the number of grey particles, normally denoted by n_g , provides an indirect measurement of the impact or collision centrality. This centrality increases with the count of grey particles. Generally speaking, n_g can be considered as the measure of violence of target fragmentation [37]. So it would be interesting to analyse the behaviour of pion with respect to n_g to gather more information about the inner dynamics of the particle production process in high-energy nuclear collision. The behaviour of pion with respect to n_g or the number of target fragments provides more insight about the chaotic behaviour of the pions in multipion production process. In this work, we have applied Visibility Graph analysis to study the fractal behaviour of multipion production in π^- -Ag/Br interactions at 350 GeV with respect to different degree of target excitation. Also, as finite number of events are available here, the use of Visibility Graph technique is justified.

The rest of the paper is organized as follows. The method of Visibility Graph technique is presented in Section 2. The details of data are given in Section 3.1. Steps of the analysis and the inferences from the test results are given in Section 3.2. The paper is concluded in Section 4.

2. Method of analysis

We would briefly describe the Visibility Graph technique and process of extracting Power of Scale-freeness of Visibility Graph, PSVG, in this section.

2.1. Visibility Graph algorithm

The Visibility Graph algorithm maps time-series X to its Visibility Graph. Suppose the vertex or node of i^{th} point of the time series is denoted by X_i . Two vertices (nodes) of the graph, X_m and X_n , are said to be connected via a bidirectional edge if and only if the below equation is valid

$$X_{m+j} < X_n + \left(\frac{n - (m + j)}{n - m} \right) (X_m - X_n), \tag{1}$$

where $\forall j \in Z^+$ and $j < (n - m)$.

In Fig. 1, it is shown that the nodes X_m and X_n , where $m = i$ and $n = i + 6$ are visible to each other only if Eq. (1) is valid. As per the Visibility Graph algorithm, two sequential points of the time series can see each other, hence all sequential nodes are connected together.

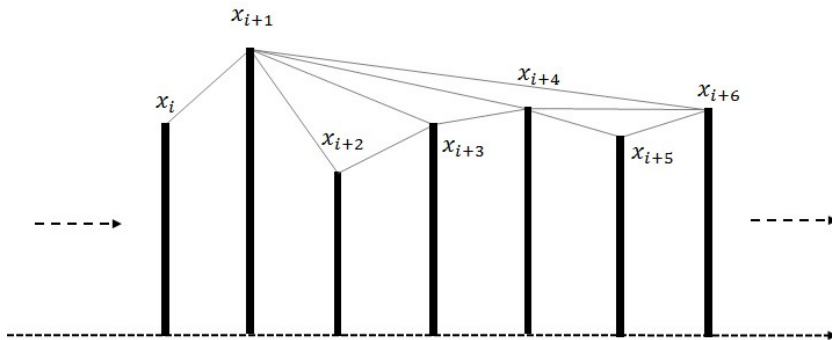


Fig. 1. Visibility Graph for time series X .

2.1.1. Power of Scale-freeness of Visibility Graph — PSVG

Lacasa *et al.* [24, 25] have confirmed that a fractal time series can be converted to a scale-free graph using Visibility Graph method. The degree of a node or vertex in a graph, here Visibility Graph, is the number of

connections or edges the node has with rest of the nodes in the graph. The degree distribution $P(k)$ of a network is then defined as the fraction of nodes with degree k , present in the network. Hence, if there are n number of nodes in total in a network and n_k of them have a degree k , we have $P(k) = n_k/n$ for all values of k . As per Lacasa *et al.* [24, 25] and Ahmadiou *et al.* [38], the degree of scale-freeness of a Visibility Graph corresponds to the amount of fractality and complexity of the time series. According to the scale-freeness property of Visibility Graph, the degree distribution of its nodes follows the power law, *i.e.* $P(k) \sim k^{-\lambda_p}$, where λ_p is a constant and it is called the Power of the Scale-freeness in Visibility Graph — PSVG. Hence, λ_p or PSVG corresponds to the amount of self-similarity, fractality and a measure of complexity of the time series.

As the fractal dimension measures the amount of self-similarity of a time series, λ_p is calculated from the slope of $\log_2[P(k)]$ versus $\log_2[1/k]$ of the time series, indicates the FD — Fractal Dimension of the signal [24, 25, 38]. It is also observed that there is an inverse linear relationship between PSVG (λ_p) and the Hurst exponent, H , of the associated time series [25].

3. Experimental details

3.1. Data description

Illford G5 emulsion plates were exposed to a π^- beam of 350 GeV incident energy from CERN, and the data used in this experiment was obtained from there. To scan the plates, a LeitzMetaloplan microscope with a specification of 10X objective lens and 10X ocular lens equipped with a semi-automatic scanning stage was used. To minimize the biases in detection, counting and measurement, each plate was scanned by two independent observers and, consequently, the scanning efficiency could be increased. An oil immersion 100X objective was used for doing the final measurement. The measuring system was integrated with both the microscopic systems having specification of 1 μm resolution along X - and Y -axes, and 0.5 μm resolution along Z -axis.

Events were selected according to the below criteria.

- The incident beam-track had to lie within 3° from the axis of the main beam in the pellicle. This criteria was to ensure the selection of real projectile beam.
- The events having the set of interactions within the range of 20 μm from top and bottom surfaces of the pellicle were rejected. This helped in reducing the losses of tracks and minimizing the errors in the measurements of both emission and azimuthal angles.

- To ensure that the events chosen should not include interactions from the secondary tracks of the other interactions, all the primary beam-tracks were traced along the backward direction

The details of the events are also elaborated in our earlier works [7, 8, 39–43]. As per the terminology of nuclear emulsion [44], the particles emitted after interactions can be classified as the shower, grey and black particles. The details of these particles are mentioned below.

1. *Shower particles.* The tracks of particles having ionization less than or equal to $1.4 I_0$ are called shower tracks, I_0 is the minimum ionization of a singly charged particle. Pions with a small admixture of K mesons and fast protons mostly generate the shower tracks. The velocities of these particles are greater than $0.7 c$, where c is the velocity of light in free space.
2. *Grey particle.* Knocked out protons in the energy range of 30–400 MeV, slow pions having energy of about 30–60 MeV, and admixture of deuterons and tritons generally produces the grey particles. They have ionization lying between $1.4 I_0$ and $10 I_0$. These grey particles have ranges greater than 3 mm in the emulsion medium and have velocities between $0.3 c$ and $0.7 c$.
3. *Black particles.* They are also known as target fragments, consisting of both singly charged and multiply charged fragments. They are fragments of various elements such as carbon, lithium and beryllium, *etc.* with ionization greater than or equal to $10 I_0$. These particles have maximum ionizing power and are less energetic and, therefore, short ranged. Their ranges are less than 3 mm in the emulsion medium. Their velocities are less than $0.3 c$.

3.2. Our method of analysis

We have divided the total number of events in three ranges of n_g . In doing so, although the number of events in some of them is comparatively low this does not affect the result of the analysis, as we have highlighted earlier in the text that this new method only can deliver reliable results with lesser data even with 400 data points [31].

To analyse the fractal behaviour of pions on target excitation, we have chosen the parameter pseudorapidity η of produced pions in π^- -Ag/Br interactions at 350 GeV and grouped the data as per the below three ranges of number of grey particles denoted by n_g . For example, the first dataset includes η values of the events having the number of grey particles n_g , in the range of $[0, 2]$ or $0 \leq n_g \leq 2$. These ranges correspond to different degree of target excitation.

1. $0 \leq n_g \leq 2$,
2. $3 \leq n_g \leq 5$,
3. $6 \leq n_g \leq 13$.

Then we have constructed Visibility Graphs from the three datasets of η values corresponding to the above three ranges of n_g , as per the method described in Section 2.1. For each of the 3 Visibility Graphs, the following parameters are analysed in Sections 3.2.1 and 3.2.2.

3.2.1. Network parameters

1. *Heterogeneity index.* This parameter calculated for the network is the quantitative characterization of network heterogeneity. Moderate to high value of this index characterizes a scale-free network. The ranges for the heterogeneity index are given in [45]. Here, heterogeneity indexes are extracted for all 3 Visibility Graphs as per the method proposed by Estrada [45] and listed in Table I. It is evident from the values that all the 3 Visibility Graphs are moderately heterogeneous. Moreover, the range of values of the indexes conforms to the scale-free property of the Visibility Graphs [45] and also it is evident that the Visibility Graph constructed for the second n_g range is the most heterogeneous.

TABLE I

Trend of heterogeneity index, average clustering coefficient, average degree for the Visibility Graphs created from the three datasets of η values corresponding to the three ranges of n_g .

n_g range	Het. index	Avg. clust. coeff.	Avg. deg.
$0 \leq n_g \leq 2$	0.23	0.64	50.16
$3 \leq n_g \leq 5$	0.26	0.63	51.97
$6 \leq n_g \leq 13$	0.24	0.61	58.80

2. *Average clustering coefficient.* This parameter measures the likelihood that whether the neighbour nodes of a node are also neighbours to each other or not. Hence, clustering coefficient of a graph is the measurement of degree towards which nodes of the graph tend to cluster together. Average clustering coefficients for the 3 Visibility Graphs are calculated as per the method prescribed by Watts and Strogatz [46] and listed in Table I. In this experiment, average clustering coefficients of the Visibility Graphs are monotonically decreasing with increasing target excitation.

3. *Average degree.* This parameter of a graph quantifies globally, what is measured locally by the node degrees of the graph [47]. Comparison of the average degree of the Visibility Graphs formed from each dataset is shown in Table I. It is evident that average degree is monotonically increasing with increasing target excitation.
4. *Average shortest path.* This parameter is defined as the average number of steps along the shortest paths for all possible pairs of network nodes. It is a measurement of the efficiency of transportation process of information through the network. The average shortest paths between the nodes of the 3 Visibility Graphs created above are calculated as per the method proposed by Johnson [48] and listed in Table II. It is the highest for the Visibility Graph created for the first range of n_g or the lowest target excitation. Then for the rest of the graphs, the values are almost similar.

TABLE II

Trend of average shortest path and assortativity coefficient for the Visibility Graphs created from the three datasets of η values corresponding to the three ranges of n_g .

n_g range	Avg. shrt. path	Ass. coeff.
$0 \leq n_g \leq 2$	3.03	-0.21
$3 \leq n_g \leq 5$	2.73	-0.21
$6 \leq n_g \leq 13$	2.74	-0.27

5. *Assortativity coefficient.* A graph is said to be assortative if its edges generally appear between its nodes of same type. It is disassortative if edges normally appear between nodes of different types. Hence, the assortativity coefficient of the Visibility Graph is the measure of correlation of degree between pairs of linked nodes. Assortativity coefficients for the Visibility Graphs are calculated as per the method proposed by Newman [49] and listed in Table II. It is evident that all the 3 graphs are disassortative. Also assortativity coefficient remains the same for the first two ranges and decreases in the third range which has the maximum target excitation.

3.2.2. Analysis of PSVG (λ_p) values

The values of $P(k)$ versus k are calculated for the Visibility Graphs corresponding to each of the three datasets as per the method described in Section 2.1.1.

The $P(k)$ versus k plot for the dataset of η values of the events having range of n_g as $0 \leq n_g \leq 2$ is shown in Fig. 2, and the power-law relationship is evident here.

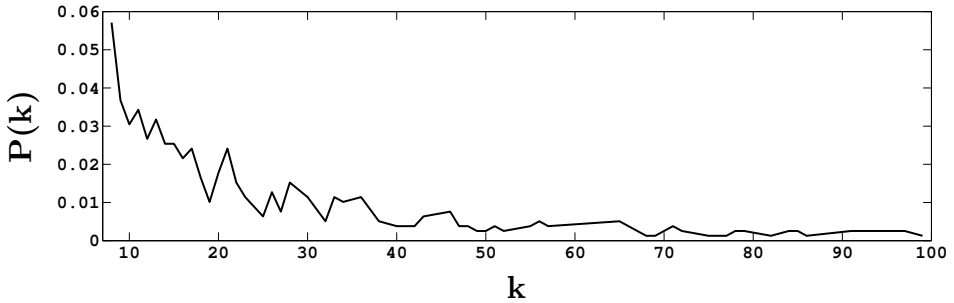


Fig. 2. $P(k)$ versus k for the Visibility Graph created for η values for the range of $0 \leq n_g \leq 2$ for π^- -AgBr interaction at 350 GeV.

PSVG (λ_p) is calculated from the slope of $\log_2[1/k]$ versus $\log_2[P(k)]$ for each set as per the method in Section 2.1.1. Plot of $\log_2[1/k]$ versus $\log_2[P(k)]$ for the range of $0 \leq n_g \leq 2$ is shown in Fig. 3. λ_p for this range is calculated as 1.37.

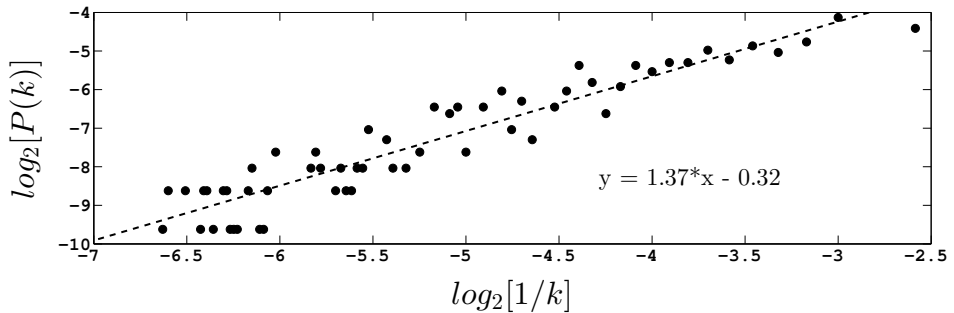


Fig. 3. Slope of $\log_2[1/k]$ versus $\log_2[P(k)]$ for the Visibility Graph created for η values for the range of $0 \leq n_g \leq 2$ for π^- -AgBr interaction at 350 GeV.

For each of the Visibility Graph constructed for the datasets of η values corresponding to 3 ranges of n_g , the λ_p values are calculated and listed in Table III. It is evident that PSVG (λ_p) is consistently decreasing with increasing ranges of n_g which signify the degrees of target excitation.

TABLE III

λ_p values calculated for n_g -range-wise datasets of η values.

n_g range	λ_p
$0 \leq n_g \leq 2$	1.37
$3 \leq n_g \leq 5$	1.23
$6 \leq n_g \leq 13$	1.18

Monte Carlo simulation for PSVG analysis

Next, we have repeated the Visibility Graph analysis as per the steps described in Section 2.1.1, on the randomized version of experimental data and calculated the values of PSVG (λ_p) and listed them in Table IV. It is evident from Table IV that PSVG values (λ_p) decrease more (around 12%) from the first to second ranges of number of grey particles (n_g) than the second to third ranges. However, λ_p decreases consistently with increase of target excitation. Further, we have generated Monte Carlo events assuming independent emission of pions in π^- -AgBr interaction at 350 GeV. Monte Carlo events have been chosen in such a way that $\frac{dn}{d\eta}$ distribution of Monte Carlo simulated events resembles the corresponding $\frac{dn}{d\eta}$ of the real ensembles. With these Monte Carlo generated events, we again repeated the same method of analysis as described in Section 2.1.1 and calculated λ_p values are listed in Table IV.

TABLE IV

λ_p values calculated for n_g -range-wise datasets of η values for experimental, randomized data and Monte Carlo generated events.

n_g range	λ_p exp	λ_p rand	λ_p mc
$0 \leq n_g \leq 2$	1.37	2.78	3.50
$3 \leq n_g \leq 5$	1.23	2.95	3.34
$6 \leq n_g \leq 13$	1.18	2.81	3.15

We can compare the PSVG (λ_p) values calculated for the:

1. Experimental data.
2. Randomized data.
3. Monte Carlo generated events.

All are listed in Table IV.

Qualitative and quantitative interpretation

From the comparison, we can state that the PSVG values for real events are substantially different from those of simulated events. The values of PSVG (λ_p) essentially is an indicator of degree of connectivity of network in a complex system. The values of λ_p in experimental data being significantly different from randomized and Monte Carlo simulated ensembles confirm that this degree of complexity, which is never the outcome of randomized or Monte Carlo simulated fluctuation pattern, is indicative of dynamics involved in pionisation process. Quantitatively the difference of λ_p , calculated for the experimental data, is of the order of 100%–140% for randomized data and 150%–170% for Monte Carlo simulated data, for all three ranges of n_g . We can get a clear picture of this difference in Fig. 4.

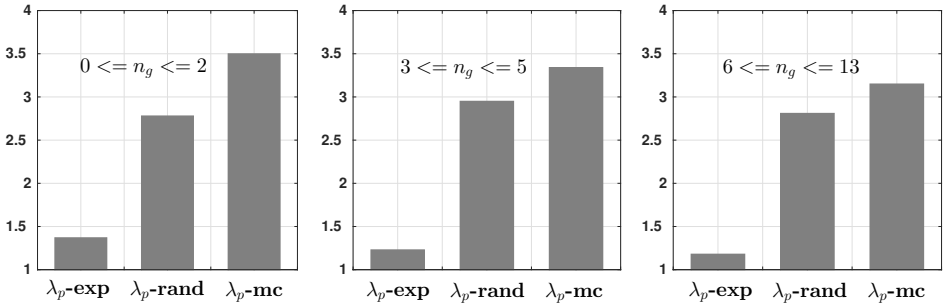


Fig. 4. Comparison of λ_p values of experimental data with randomized and Monte Carlo generated events, for each n_g range.

It is relevant to analyse the origin of strong difference of PSVG parameters of experimental data with randomized and Monte Carlo simulated data. To provide order or definite properties to a structural form inherent in the chaos-based complex system, fractal geometry has been evolved. In the case of Visibility Graph method, the data series in question is converted to a graph and, as per Lacasa *et al.* [24, 25], a fractal data series is always converted to a scale-free graph [24]. As power-law relationship between two quantities represents self-similarity of the large and small fragments of a fractal system, we can deduce that the power-law relationship visible in degree distribution series derived from the Visibility Graph constructed from the data series, confirms the graph’s scale-freeness property which has been inherited from the data series. As already explained in Section 2.1.1, this power-law exponent or the PSVG parameter corresponds to the amount of complexity and fractality of the data series and, in turn, indicates the fractal dimension of the data series [24, 25, 38]. Hence, PSVG (λ_p) provides a measure of degree of complexity and, therefore, with the help of this parameter, one can characterise dynamics behind a complex phenomenon. Further,

there exists an inverse linear relationship between λ_p and the Hurst exponent and, as mentioned earlier in the manuscript, the visibility graph technique is more suitable for accurately finding the Hurst exponent [25]. We can also use the Hurst exponent to compare between experimental data and randomized and Monte Carlo simulated data. Figure 5 shows strong values of the Hurst exponent of experimental data compared to that of randomized and Monte Carlo simulated data, justifiably opposite to the behaviour shown by PSVG analysis in Fig. 4.

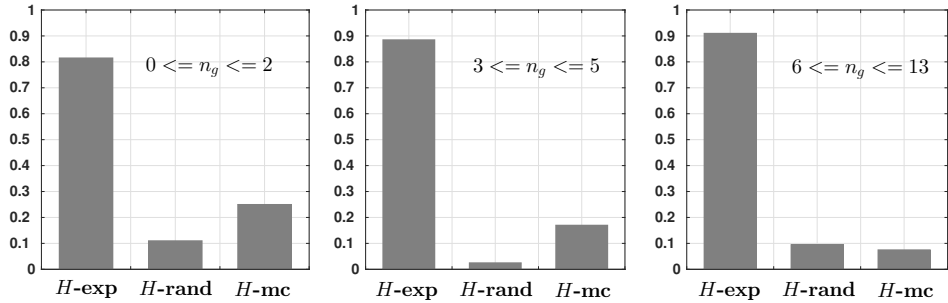


Fig. 5. Comparison of Hurst exponent values of experimental data with randomized and Monte Carlo generated events, for each n_g range.

The Hurst exponent can decipher information about short-range correlation [13]. Thus, PSVG values reveal the degree of complexity involved, whereas the Hurst exponent provides information about the degree or nature of short-range correlation. Needless to say, the trends of both the parameters show that the dynamics of pion fluctuations studied cannot be accounted for randomness or fluctuations of Monte Carlo simulated events. In short, the experimental data used for fluctuation studies, when compared with random/Monte Carlo simulated data may show smaller/larger values according to the specifics of the parameters (PSVG/Hurst exponent) revealing identical information about inner dynamics.

Thus, using this novel approach of complex network based method, high-energy pionisation process can be studied quantitatively exploiting a new parameter λ_p , *i.e.* PSVG (along with the Hurst exponent derived from PSVG). PSVG can be useful not only for assessment of degree of fluctuation in different nuclear collisions but also for assessment of prospective phase transition. One single quantitative parameter, λ_p , suffices to decode the dynamics of pionisation process in high-energy interaction using a more precise and robust methodology.

4. Conclusion

- We have presented a chaos-based rigorous non-linear technique called Visibility Graph analysis (utilizing the parameters — heterogeneity index, average clustering coefficient, degree and shortest path, assortativity coefficient and PSVG (λ_p)), to study the fluctuation of pions in high-energy collision. In this analysis, we have studied π^- -Ag/Br interactions at 350 GeV using Visibility Graph analysis.
- This work presents new data on scaling behaviour of multiplicity fluctuations from a new perspective. As evident from figures and tables, the study clearly indicates that the pion multiplicity fluctuations obey a scaling law. Further, we have found a decreasing trend of PSVG values (λ_p) for three ranges of grey particles (n_g) confirming that the fractal behaviour of pion production decreases with increase of target excitation. This is an interesting and useful finding in the case of hadron–nucleus interaction at high energy.
- The study of scaling behaviour from an entirely new perspective is a first of the kind analysis in the domain of high-energy pionisation process yielding interesting, reliable results useful for understanding the dynamics of pion production in high-energy hadronic and nuclear interaction.
- Similar analysis can be done with the hadronic data of high energy and result would be of immense importance for modelling pionisation process in high-energy nuclear collision. Eventually, we emphasize the assessment of phase transition in high-energy collision, with the help of network analysis, exploiting the PSVG (Power of the Scale-freeness in Visibility Graph, which is implicitly connected with the Hurst exponent. The Hurst exponent has recently been confirmed as a good indicator of phase transition for magnetization time series [32]). This analysis can be extended with ALICE data of Pb–Pb collision and, in future experiments, with high energies to capture the onset of QGP.

We thank the Department of Higher Education, Government of West Bengal, India for logistics support of computational analysis.

REFERENCES

- [1] A. Bialas, R. Peschanski, *Nucl. Phys. B* **273**, 703 (1986).
- [2] R. Hwa, *Phys. Rev. D* **41**, 1456 (1990).
- [3] G. Paladin, A. Vulpani, *Fractals* **3**, 785 (1995).

- [4] P. Grassberger, *Physica D* **13**, 34 (1984).
- [5] T.C. Halsey *et al.*, *Phys. Rev. A* **33**, 1141 (1986).
- [6] F. Takagi, *Phys. Rev. Lett.* **72**, 32 (1994).
- [7] D. Ghosh, A. Deb, M. Lahiri, *Phys. Rev. D* **51**, 3298 (1995).
- [8] D. Ghosh, A. Deb, S. Bhattacharyya, U. Datta, *J. Phys. G: Nucl. Part. Phys.* **39**, 035101 (2012).
- [9] C.K. Peng *et al.*, *Phys. Rev. E* **49**, 1685 (1994).
- [10] J.W. Kantelhardt *et al.*, *Physica A* **295**, 441 (2001).
- [11] M.S. Taqqu, V. Teverovsky, W. Willinger, *Fractals* **3**, 785 (1995).
- [12] Z. Chen, P.Ch. Ivanov, K. Hu, H.E. Stanley, *Phys. Rev. E* **65**, 041107 (2002).
- [13] J.W. Kantelhardt *et al.*, *Physica A* **316**, 87 (2002).
- [14] Y.X. Zhang, W.Y. Qian, C.B. Yang, *Int. J. Mod. Phys. A* **23**, 2809 (2008).
- [15] D. Ghosh *et al.*, *Phys. Rev. C* **65**, 067902 (2002).
- [16] D. Ghosh *et al.*, *Fractals* **13**, 325 (2005).
- [17] E.G. Ferreira, C. Pajares, *Phys. Rev. C* **86**, 034903 (2012).
- [18] S. Dutta, D. Ghosh, S. Chatterjee, *Int. J. Mod. Phys. A* **29**, 1450084 (2014).
- [19] P. Mali *et al.*, *Physica A* **424**, 25 (2015).
- [20] R. Albert, A.L. Barabási, *Rev. Mod. Phys.* **74**, 47 (2002).
- [21] A.L. Barabási, *Nature Phys.* **8**, 14 (2012).
- [22] S. Havlin, *Eur. Phys. J. Spec. Top.* **214**, 273 (2012).
- [23] L. Zhao, W. Li, X. Cai, *Phys. Lett. A* **380**, 654 (2016).
- [24] L. Lacasa *et al.*, *Proc. Natl. Acad. Sci.* **105**, 4972 (2008).
- [25] L. Lacasa, B. Luque, J. Luque, J.C. Nuno, *Europhys. Lett.* **86**, 30001 (2009).
- [26] D. Hofstadter, *Gödel, Escher, Bach: An Eternal Golden Braid*, Vintage Books, NY 1980.
- [27] M.A. Stern, *Ueber eine zahlentheoretische Funktion*, *Journal für die reine und angewandte Mathematik* **55**, 193 (1858).
- [28] M. Schroeder, *Fractals, Chaos, Power Laws: Minutes from an Infinite Paradise*, New York: W.H. Freeman, 1991.
- [29] J.M. Hausdorff, *J. Appl. Physiol.* **80**, 1448 (1996).
- [30] A.L. Goldberger *et al.*, *Proc. Natl. Acad. Sci.* **99**, 2466 (2002).
- [31] S. Jiang, C. Bian, X. Ning, Q.D.Y. Ma, *Appl. Phys. Lett.* **102**, 253 (2013).
- [32] L. Zhao *et al.*, *PLoS ONE* **12**, e0170467 (2017).
- [33] S. Bhaduri, D. Ghosh, *Int. J. Mod. Phys. A* **31**, 1650185 (2016).
- [34] S. Bhaduri, D. Ghosh, *Mod. Phys. Lett. A* **31**, 1650158 (2016).
- [35] S. Bhaduri, D. Ghosh, *Adv. High Energy Phys.* **2016**, 6848197 (2016).
- [36] A. Bhaduri, S. Bhaduri, D. Ghosh, "Azimuthal Pion fluctuation in Ultrarelativistic Nuclear Collisions and centrality dependence — A Study with Chaos based Complex Network Analysis", *J. Phys. Part. Nuclei Lett.*, 2016, in press,

- [37] B. Andersson, I. Otterlund, E. Stenlund, *Phys. Lett. B* **73**, 343 (1978).
- [38] M. Ahmadlou, H. Adeli, A. Adeli, *Physica A* **391**, 4720 (2012).
- [39] D. Ghosh, P. Ghosh, A. Ghosh, J. Roy, *Phys. Rev. C* **49**, R1747 (1994).
- [40] D. Ghosh *et al.*, *Phys. Rev. C* **59**, 2286 (1999).
- [41] D. Ghosh, A. Deb, S.R. Sahoo, P.K. Haldar, *Europhys. Lett.* **56**, 639 (2001).
- [42] D. Ghosh, A. Deb, M. Mondal, J. Ghosh, *Phys. Lett. B* **540**, 52 (2002).
- [43] D. Ghosh, A. Deb, S. Bhattacharyya, U. Datta, *Pramana* **77**, 297 (2011).
- [44] C.F. Powell, P.H. Fowler, D.H. Perkins, *The Study of Elementary Particles by the Photographic Method*, Pergamon Press, Oxford 1959.
- [45] E. Estrada, *Phys. Rev. E* **82**, 066102 (2010).
- [46] D.J.J. Watts, S.H.H. Strogatz, *Nature* **393**, 440 (1998).
- [47] S.C. Carlson, *Encyclopaedia Britannica*, 2014, *Graph Theory*, <https://www.britannica.com/topic/graph-theory>
- [48] D.B. Johnson, *JACM* **24**, 1 (1977)
- [49] M.E.J. Newman, *Phys. Rev. Lett.* **89**, 208701 (2002).